Atomic Structure of Pyramidal Defects in GaN:Mg; Influence of Annealing

Z. Liliental-Weber, T. Tomaszewicz, D. Zakharov, and M. O'Keefe
Lawrence Berkeley National Lab, Berkeley, CA 95720, USA

S. Hautakangas and K. Saarinen
Laboratory of Physics, Helsinki University of Technology, 02015 HUT, Finland

J. A. Freitas
ESTD-Electronic Materials Branch, Naval Research Laboratory, Washington, D.C. 20375, USA

Abstract:

The atomic structure of the characteristic defects (Mg-rich hexagonal pyramids) in p-doped bulk and MOCVD GaN:Mg thin films grown with Ga polarity was determined at atomic resolution by direct reconstruction of the scattered electron wave in a transmission electron microscope. Small cavities were present inside the defects, confirmed also with positron annihilation. The inside walls of the cavities were covered by GaN of reverse polarity compared to the matrix. Defects in bulk GaN:Mg were almost one order of magnitude larger than in thin films. An exchange of Ga and N sublattices within the defect compared to the matrix lead to a 0.6±0.2Å displacement between the Ga sublattices of these two areas. A [1100]/3 shift with change from AB stacking in the matrix to BC within the entire pyramid was observed. Annealing of the MOCVD layers lead to slight increase of the defect size and an increase of the photoluminescence intensity. Positron annihilation confirms presence of vacancies of different sizes triggered by the Mg doping in as-grown samples and decrease of their concentration upon annealing at 900 and 1000°C.

1. Introduction

P-doping of GaN remains still difficult and not well understood. Mg remains the most efficient p- dopant but the free hole concentration is limited to $2x10^{18}cm^{-3}$ for Mg concentrations in the low $10^{19}cm^{-3}$ range. This could limit further development of GaN based devices. Further increase of the Mg concentration, up to $1x10^{20}cm^{-3}$ leads to a decrease of the free hole concentration. This is commonly interpreted as auto-compensation due to increased formation of N vacancies or vacancy complexes with Mg [1]. Another characteristic feature is the occurrence of the so-called "blue band" in the photoluminescence spectra of highly Mg-doped GaN grown by MOVPE [2].

2. TEM studies of defects in bulk and MOCVD grown GaN:Mg layers

Transmission electron microscopy (TEM) studies show the formation of different types of Mg–rich defects, both in bulk crystals grown from Ga excess under high N-pressure and in crystals grown by MOCVD [3-6]. The types of the defects strongly depend on crystal growth polarity. For bulk crystals grown with N-polarity, the planar defects are distributed at equal distances (20 unit cells of GaN). These defects were described as inversion domains [6].

For growth with Ga-polarity (for both bulk and MOCVD grown crystals) Mg-rich pyramidal defects have been found when Mg concentration reaches about $1x10^{20}cm^{-3}$[4-6].

Majority of them are three-dimensional Mg-rich hexagonal pyramids with their base on the (0001) plane and six walls formed on {11$\underline{2}$3} planes (Fig. 1a). Some of them are truncated pyramids with longer and shorter bases formed on c-planes with the walls formed on the same planes (Fig. 1b). These pyramids and truncated pyramids cannot be distinguished in plan-view configuration indicating their common origin (Fig.1 c-f). It appears that the dimension of these pyramids varies depending on growth method, but the angle between the base and their sides remain the same. In the bulk crystals the diameter of the base can be almost one order of magnitude larger (up to 1000 Å) than in thin foils grown by MOCVD (30Å-150Å). Our studies show formation of small Ga/Mg clusters near the tip of the pyramid [7]. It is possible that such clusters are origins of these defects. It is possible that depending on the cluster size the defect develops either in a pyramid or truncated pyramid.

These both defects have often holes in their centers and are decorated by Mg on the defect walls [4-5]. Presence of such holes was also confirmed by positron annihilation study [7]. Since these defects were also described as inversion domains [8] or Mg_3N_2 precipitates [9] high resolution focal series for focal-series reconstruction of the electron exit-surface wave (ESW) leaving the specimen were applied for these studies [10].

Reconstructed exit wave phase from the area close to the pyramid tip (Fig. 2) showed blobs with two distinct intensity peaks, identified as due to Ga and N atomic columns. Using Argand plots [11, 12], we confirmed that the phase of atoms described as Ga gave the highest peak, followed by a smaller phase peak described as N, as expected from earlier theoretical calculations [13]. This identification of the atomic positions of Ga and N from the experimental reconstructed exit wave confirmed inversion of polarity within the pyramid compared to the matrix. In addition, it showed that AB stacking in the matrix changes to BC stacking within the pyramid (Figs. 2b-d). This stacking arrangement holds through the entire pyramid and changes back to the AB stacking order above the pyramid base (Fig. 3). Analysis of the reconstructed exit wave phase image from the pyramid side (along c planes) indicates a shift of Ga atomic column positions from the matrix to the N position within the pyramid. In this way a 0.6Å±0.2Å displacement can be measured on the pyramid side between Ga positions in the matrix and within the pyramid (Fig. 4).

Decoration by Mg was observed on the defect base and defect walls but not further from these interfaces excluding formation of Mg_3N_2 precipitates suggested earlier [9]. Analysis of reconstructed exit wave phase on the defect base shows that N positions were occupied by different type of atoms. Since these atomic columns had phases smaller than the surrounding Ga columns above the base, they could be due to the presence of Mg in this part of defect. This is consistent with a larger separation between c-planes measured across the base. Increase in separation starts at 0.2Å above the pyramid and can grow, in some cases, up to 0.6Å at the pyramid base (see Fig. 3).

3. Annealing of GaN:Mg

We were also studied correlation between the structure, photoluminescence and positron annihilation for as-grown and annealed samples. The MOCVD samples 1900Å thick were annealed at 900°C and 1000°C. TEM studies of as-grown samples show formation of small Mg-rich clusters and pyramids with their diameter (e.g. length of their bases) in the range of 25-35Å

where larger sizes were easy to observe only about 600-800Å from the sample surface and deeper. Annealing at 900°C did not change substantially the size of the pyramid bases and measured lengths were very close to 35Å, but the small clusters in subsurface areas have been not observed. However, annealing at 1000°C lead to slight increase of the pyramid sizes to about 35-45Å. They were much easier recognizable already in the subsurface area and the larger sizes about 100 nm from the sample surface. The distance between pyramids in the annealed samples was larger than between the clusters (or small pyramids) in the as-grown samples. The density of these pyramids in the 1000°C annealed samples was estimated to be between 10^{16}- 10^{17}cm^{-3} observed in cross-section samples. It is expected that the density of these defects in as-grown samples (taking also into account clusters) would be in high 10^{17}cm^{-3} range, however it was also noticed that distribution of these pyramids changes substantially in different areas of each sample. This applies to both as-grown and annealed samples. Especially in as-grown samples the smallest defects were difficult to count.

Positron annihilation spectroscopy was applied to investigate native defects in Mg-doped GaN films. The method is an effective tool for studying vacancy type defects in semiconductors. Because of the positron charge, the region of the sample where the positive background is reduced can be found, and hence the positrons are trapped by negative and neutral vacancies due to the missing positive ion core. The trapping increases the lifetime of the positron and narrows the momentum distribution of the positron-electron pair. The energy distribution of annihilated positron-electron pairs was characterized by S and W parameter [15]. The S parameter represents annihilations with valence electrons with longitudinal momentum component and W parameter describes the annihilations with high momentum core electrons. At a vacancy the electron momentum is locally decreased, which leads to the narrowing of the energy distribution of annihilation photons. Fig. 5a shows the S parameter as a function of incident positron energy in Mg-doped GaN samples before and after thermal annealing and compared to the vacancy free parameter level in GaN, which is well known on the basis of previous studies [15-17].

In the unannealed GaN:Mg layer (50-1000 nm) S parameter is bigger than the reference level indicating positron trapping at vacancy type defects. The increase of S parameter after 50 nm is due to the increased vacancy concentration in the layer. This kind of inhomogeneous defect profile is studied carefully in a very recent publication with positron lifetime and Doppler spectroscopy, where the profile is connected to inhomogeneous vacancy cluster concentration [18]. The detailed positron lifetime measurement reveals also monovacancy-type defects in the unannealed GaN:Mg layers [15,18]. According to these measurements the inhomogeneous defect profile of GaN:Mg layer is arising from vacancies of different sizes, which is triggered by the Mg doping . Positron lifetime larger than 500 ps (180 ps in the vacancy free samples) was associated with large vacancy clusters, consistent with the areas where pyramidal defects have been found confirming TEM results of the presence of holes within these pyramids [7]. After annealing at 900°C and 1000 °C the defect profile is homogeneous and their concentrations is decreased close to the detection limit (10^{16}cm^{-3}). Thermal treatment makes the vacancy defects positive by dissociation of defect complexes [18]. On the other hand the migration should play a crucial role at these annealing temperatures leading to vacancy diffusion to the surface.

Photoluminescence (PL) has proven to be a powerful, sensitive, non-destructive technique for the detection and identification of impurities and other defects in semiconductors. Electrons and holes optically excited across the forbidden energy gap usually become localized or bound at an impurity or defect before recombining. The identity of the localized center to

which they are bound can often be determined on the basis of the binding energies inferred from the spectral positions or from thermal quenching studies. Qualitative information about crystal quality can be accessed from the efficiency and line widths of near band edge PL spectra. A broad scope of phenomena such as excitation, recombination mechanism, structural defects, and impurities can be investigated. In general, a number of defects present simultaneously in the material can compete at different rates for the photo-excited carriers resulting in radiative or non-radiative recombination processes. Therefore, PL is not adequate to verify the concentration of defects.

The PL measurements were carried at room temperature on the same MOCVD grown samples on which later positron annihilation and finally TEM studies have been performed. The samples luminescence, excited with the 325 nm HeCd laser line, were dispersed by a double-grating spectrometer fitted with an UV-sensitive GaAs photomultiplier and a computer controlled photon-counter. The spectrometer calibration was verified with standard lines from a mercury calibration lamp.

In Fig. 5b we show the room temperature PL spectra of an unannealed, and annealed at 900^{o}C and 1000^{o}C GaN:Mg samples, originated from the same 2" wafer. Note the increase of the PL band intensity with increasing annealing temperature. This emission band intensity increase has been attributed to the increasing of the concentration of thermal-activated Mg impurities. The energy position of this band is associated with the recombination process involving a deep donor and the Mg acceptor [19, 20]. This would be consistent with TEM observation of disappearance of small Mg-rich clusters and would show that not all Mg was consumed by the formation of pyramidal defects.

4. Summary

Transmission electron microscopy and reconstructed exit wave phase imaging were applied to study defects formed in bulk and MOCVD GaN:Mg crystals grown with Ga polarity. Two types of defects have been found: hexagonal pyramids with 6 inclined walls and a base formed on c-plane, and truncated pyramids. These defects have a hollow core, but their walls are covered by a substantial thickness of GaN grown with opposite polarity. Positron annihilation confirms the presence of large vacancy clusters. Annealing of GaN:Mg MOCVD layers lead to disappearance of Mg rich clusters and slight increase of pyramid sizes at 1000°C. Much more pyramidal defects have been found in the subsurface area for the 1000°C annealing temperature. PL data show also some increase of intensity, suggesting increased concentration of thermally activated Mg.

Acknowledgment:

This work was supported by the U.S. Department of Energy under contract DE-AC03-76SF00098. Use of the OÅM facility at the National Center for Electron Microscopy at the LBNL is greatly appreciated.

References:

1. U. Kaufman, P. Schlotter, H. Obloch, K. Kohler, M. Maier, Phys. Rev. **B62**, 10867 (2002).
2. S. Nakamura and G. Fasol, *"The blue laser diode"* (Springer-Verlag, Berlin (1997).
3. Z.Liliental-Weber, M. Benamara, J. Washburn, et al, Phys. Rev. Letter. **82**, 2370 (1999).
4. Z. Liliental-Weber, M. Benamara, W. Swider, J. Washburn, I. Grzegory, S. Porowski, R.D. Dupuis, and C.J. Eiting, Physica B **273-274**, 124 (1999).
5. Z. Liliental-Weber, M. Benamara, J. Washburn, I. Grzegory, S. Porowski, D.J.H. Lambert, C.J. Eiting, and R.D. Dupuis, Appl. Phys. Lett. **75**, 4159 (1999).
6. Z. Liliental-Weber, J. Jasinski, M. Benamara, I. Grzegory, S. Porowski, D.J.H. Lambert, C.J. Eiting, and R.D. Dupuis, Phys. Stat. Sol. (b) **228**, No. 2, 345 (2001).
7. Z. Liliental-Weber, T. Tomaszewicz, D. Zakharov, J. Jasinski, M.A. O'Keefe, S. Hautakangas, A. Laakso, and K. Saarinen, Mat. Res. Symp. Proc. 798, 711 (2004).
8. P. Vennegues, M. Leroux, S. Dalmasso, M. Benaissa, et al. Phys. Rev. B 68, 235214 (2003).
9. D.P. Bour, H.F. Chung, W. Gotz, L. Romano et al, Mater. Res. Soc. Symp. **449**, 509 (1997).
10. A. Thust, W.M.J. Coene, M. Op De Beeck, and D. Van Dyck, Ultramicroscopy **64**, 211 (1996).
11. Argant plot D. Van Dyck and M. Op De Beeck, Ultramicroscopy **64**, 99 (1996).
12. W. Sinkler and L. D. Marks Ultramicroscopy **75**, 251 (1999).
13. Z. Liliental-Weber, T. Tomaszewicz, D. Zakharov, J. Jasinski, and M.A. O'Keefe, Phys. Rev. Lett. **93**, 206102 (2004).
14. K. Saarinen, P. Hautojarvi and C. Corbel, in "Identification of Defects in Semiconductors", (Academic Press, New York) (1998)
15. S. Hautakangas, J. Oila, M. Alatalo, K. Saarinen, L. Liszkay, D. Seghier, and H. P. Gislason, Phys. Rev. Lett., **90**, 137402 (2003).
16. J. Oila, V. Ranki, J. Kivioja, K. Saarinen, P. Hautojarvi, J. Likonen, J. M. Baranowski, K. Pakula, T. Suski, M. Leszczynski, and I. Grzegory, Phys. Rev. B., **63**, 045205 (2001).
17. P. Laukkanen, S. Lehkonen, P. Uusimaa, M. Pessa, J. Oila, S. Hautakangas, K. Saarinen, J. Likonen, and J. Keranen, J. Appl. Phys., **92**, 786 (2002).
18. S. Hautakangas, K. Saarinen, L. Liszkay, J. Freitas, Jr., R. L. Henry, Phys. Rev. B , (2005) in print.
19. A.E. Wickenden, L.B. Rowland, K. Doverspike, D.K. Gaskill, J.A. Freitas, Jr., D.S. Simons, and P.H. Chi, *J. Electron. Mater.,* **24** (1995) 1547.
20. H.Teisseyre, T. Suski, P. Perlin, I. Grzegory, M. Leszczynski, M. Bockowski, S. Porowski, J.A. Freitas, Jr., R.L. Henry, A.E. Wickenden, and D.D. Koleske, *Phys. Rev. B* **62** (2000) 10151.

Figure Caption:

Fig. 1. TEM micrographs of two types of defects observed in cross-section samples: (a) a pyramid seen as triangular defect, (b) a truncated pyramid is seen as a trapezoid. (c-f) Same defects observed in plan-view samples. Their shapes indicate different sectioning in the plan-view TEM sample.

Fig. 2. Cross-section image from the part of pyramid close to the pyramid tip, schematically shown as inset in (a), (b) reconstructed exit wave phase from the side interface: P-inside the pyramids, I-the side interface area, M-the matrix below the side interface, (c) and (d) magnified reconstructed exit wave phase from the marked areas shown in (b) from the pyramid and the matrix, respectively, in high magnification with indicated atom position. Note stacking change within the defect (BC) compared to the matrix (AB).

Fig. 3. Reconstructed exit wave phase from the area surrounding a pyramid base. Large and small circles indicate Ga and N atomic columns. At the base these columns were impossible to distinguish and atomic columns are only marked by one circle. This observation is consistent with the presence of double Mg layer on the base of the defect. The expansion between c-planes is indicated on the right side. Note N-polarity within the defect (lower part of the micrograph) and Ga-polarity above the base (upper part of the micrograph).

Fig. 4. (a) Reconstructed exit wave phase image from the pyramid side (a higher magnification from the box marked on the schematic in the upper left corner; (b) reconstructed exit wave phase image from the larger area of the pyramid (schematically showed on the inset). Note hole present in the lower left corner; (c) and (d) very high magnification of the reconstructed wave phase image from the pyramid and from the matrix close to the pyramid side, respectively, aligned along one c-plane, together with marked atomic columns. Note that Ga positions in the matrix exchange positions with the N atomic columns within the defect leading to 0.6Å displacement between Ga sublattices within the pyramid and in the matrix.

Fig. 5(a). Positron annihilation from the as-grown and annealed samples. Note decrease of S parameter in the annealed samples and an increase of W parameter. (b) Room temperature PL spectrum of an unannealed, and annealed at 900^{o}C and 1000^{o}C GaN:Mg samples, originated from the same wafer showing an intensity increase upon annealing. The variation of the interference fringe positions results from small variations on the film thicknesses. The absence of near band-edge emission is consistent with the high concentration of Mg acceptors.

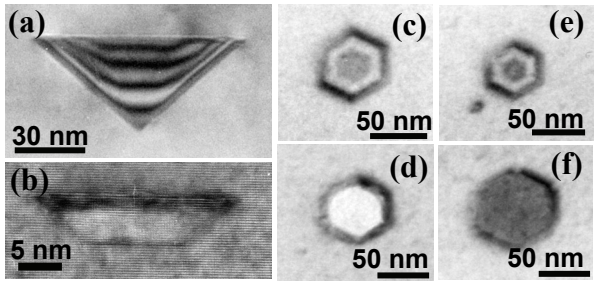

Fig. 1

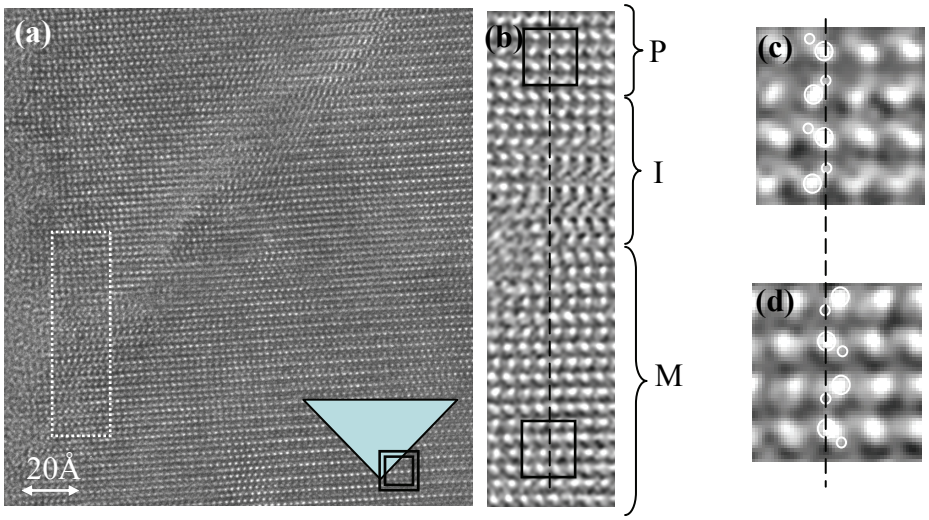

Fig. 2

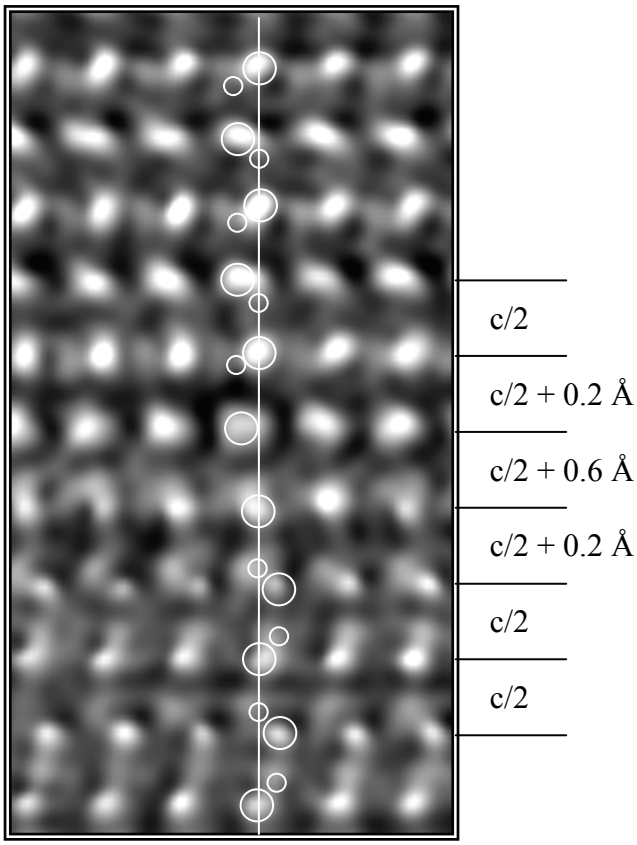

Fig. 3.

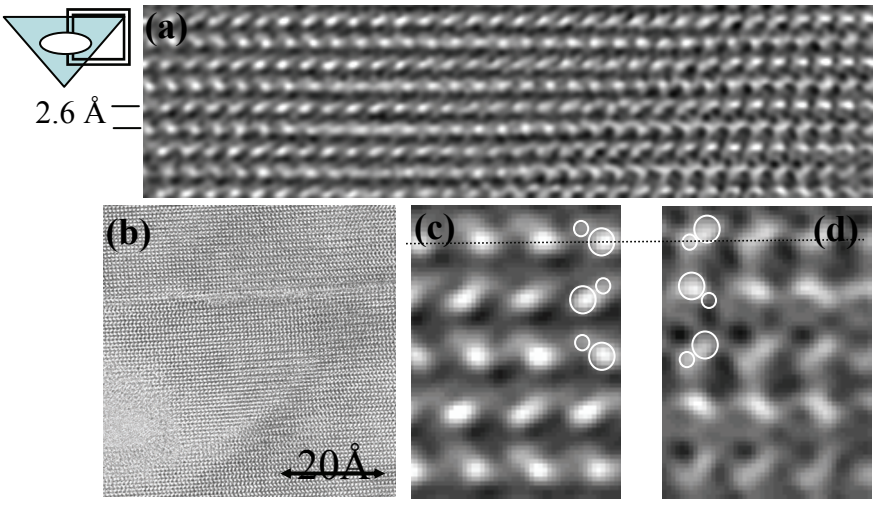

Fig. 4

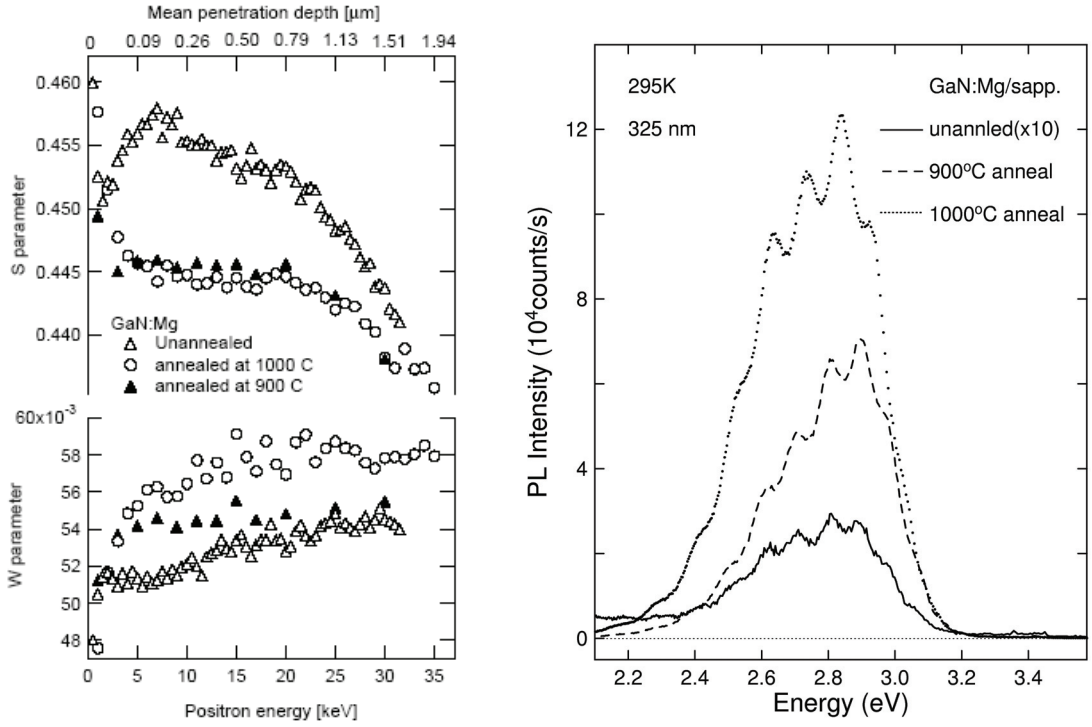
Mean penetration depth [μm]
0 0.09 0.26 0.50 0.79 1.13 1.51 1.94
S parameter
GaN:Mg
Unannealed
annealed at 1000 C
annealed at 900 C
W parameter
Positron energy [keV]
295K
325 nm
GaN:Mg/sapp.
unannled(x10)
900ºC anneal
1000ºC anneal
PL Intensity (10^4counts/s)
Energy (eV)

Fig. 5.